LOCKHEED MARTIN ENERGY RESEARCH LIBRARIES
3 4456 0514423 3

CENTRAL RESEARCH LIBRARY
DOCUMENT COLLECTION

OAK RIDGE NATIONAL LABORATORY
operated by
UNION CARBIDE CORPORATION • NUCLEAR DIVISION
for the
U. S. ATOMIC ENERGY COMMISSION

ORNL - TM - 3523

Cy 1

FAILURE OF ALUMINUM TUBING IN THE ORNL 86-INCH CYCLOTRON

R. T. King
E. L. Long, Jr.
M. R. Skidmore
J. E. Beaver

OAK RIDGE NATIONAL LABORATORY
CENTRAL RESEARCH LIBRARY
DOCUMENT COLLECTION
LIBRARY LOAN COPY
DO NOT TRANSFER TO ANOTHER PERSON
If you wish someone else to see this document, send in name with document and the library will arrange a loan.
UCN-7969
(3 3-67)

NOTICE This document contains information of a preliminary nature and was prepared primarily for internal use at the Oak Ridge National Laboratory. It is subject to revision or correction and therefore does not represent a final report.

This report was prepared as an account of work sponsored by the United States Government. Neither the United States nor the United States Atomic Energy Commission, nor any of their employees, nor any of their contractors, subcontractors, or their employees, makes any warranty, express or implied, or assumes any legal liability or responsibility for the accuracy, completeness or usefulness of any information, apparatus, product or process disclosed, or represents that its use would not infringe privately owned rights.

ORNL-TM-3523

Contract No. W-7405-eng-26

METALS AND CERAMICS DIVISION
ISOTOPES DIVISION

FAILURE OF ALUMINUM TUBING IN THE ORNL 86-INCH CYCLOTRON

R. T. King
E. L. Long, Jr.
M. R. Skidmore
J. E. Beaver

OCTOBER 1971

OAK RIDGE NATIONAL LABORATORY
Oak Ridge, Tennessee
operated by
UNION CARBIDE CORPORATION
for the
U.S. ATOMIC ENERGY COMMISSION

LOCKHEED MARTIN ENERGY RESEARCH LIBRARIES
3 4456 0514423 3

CONTENTS

	Page
Abstract	1
Introduction	1
Specimen History, Preparation, and Results	1
Discussion	6
Solution to the Problem	11
Conclusions	12
Acknowledgments	12
References	13

FAILURE OF ALUMINUM TUBING IN THE ORNL 86-INCH CYCLOTRON

R. T. King
E. L. Long, Jr.
M. R. Skidmore*
J. E. Beaver†

ABSTRACT

An internally pressurized 1100 aluminum tubular component of the ORNL 86-in. cyclotron fails periodically as a result of 22.5 MeV proton bombardment. The ion bombardment creates displacement damage and deposits hydrogen gas which forms bubbles in the tube wall. Accelerated erosion of the tube and failure occur in the region where the bubbles are observed.

INTRODUCTION

The behavior of hydrogen in aluminum has been studied in the past by numerous investigators who have been concerned with blistering and gas bubble formation during casting.[1] More recently, it has been shown that cyclotron-injected hydrogen affects the rate at which voids form in aluminum during neutron irradiation at elevated temperatures.[2]

This paper deals with the failure of 1100 aluminum tubing under a circumstance which is perhaps unique to cyclotron operation, where very high concentrations of hydrogen may be injected into a component. However, it may also have some relevance to neutron irradiation problems, to ion engines, and even to space craft which operate for long times at high velocities in regions of relatively high hydrogen concentration.

SPECIMEN HISTORY, PREPARATION, AND RESULTS

The beam extraction system of the ORNL 86-in. cyclotron has a ladder-like electrostatic deflector which is used to extract and control the direction of flight of protons. The individual rungs are flattened

*Isotopes Division, Electro Magnetic Separation Department.

†Now with University of Miami Medical School, Department of Nuclear Medicine, Miami, Florida 33100.

1100 aluminum tubes through which coolant water flows. The first rung of the ladder intercepts a variable current of 22.5 MeV protons, on the order of 10 μa, creating marketable transmutation-produced isotopes. However, the first rung often fails without warning, releasing its coolant inside the main cyclotron chamber through "pinhole leaks." The time to failure depends upon the exact operating parameters of the cyclotron, but it is usually several thousand hours of operation.

One such flattened tube, which had undergone a long period of service, was shipped to the Metals and Ceramics Division of ORNL to analyze the cause of failure and to attempt to determine whether the problem might be avoided in the future. A cross section was taken through the tube and examined metallographically. A second specimen was taken from a slightly different location and annealed for 20 hr at 600°C prior to a metallographic examination.

The appearance of a section through the unannealed tube is shown in Fig. 1. The approximate angle of incidence of the bean to the flattened section of the tube (approx 10°) is shown to illustrate three paths which protons incident upon the tube might follow. Paths 1 and 3 are through aluminum only. Path 2 involves ion deceleration by both aluminum and water. The range of a 22.5 MeV proton in aluminum[3] is approximately 0.26 cm, which is the distance measured from the front edge of the tube to the point where noticeable surface roughening first occurs on the inside surfaces of the tube (left side of rough area) along Path 1 and Path 3. A proton following Path 2 passes through about 0.07 cm of aluminum before entering the coolant, degrading its energy from 22.5 to 18.8 MeV. The range of an 18.8 MeV proton in H_2O is approximately 0.37 cm, which would allow particle passage almost to the end of the roughened lower inner surface along Path 2. The roughened surface is ascribed to the presence of injected gas, a point which will be demonstrated below. Since the path-length straggling of 22.5 MeV protons in aluminum is on the order of 1% (much smaller than the total roughened area),[3] the deflection system must have been operated in several attitudes at beam incidence angles greater than 10°.

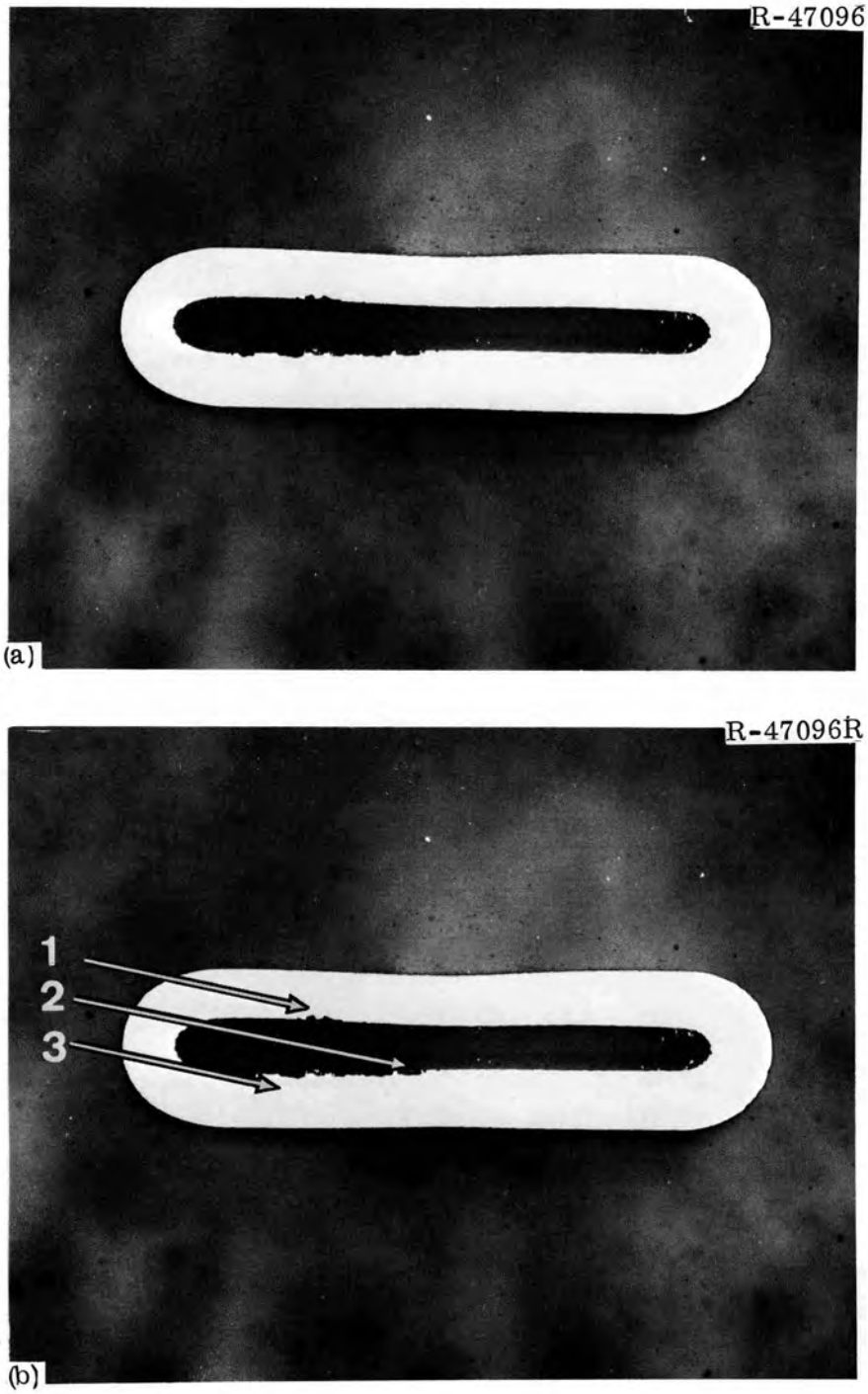

Fig. 1. Appearance of a Transverse Section Through a Flattened Tube From the Extraction System of the ORNL 86-in. Cyclotron. 10×. (a) General appearance and (b) location of proton paths.

Figure 2 shows the microstructure of the upper half of the as-bombarded tube at higher magnifications. At 100× (Fig. 2), two unusual features are observed: (1) a dark band runs from the lower left to the upper right of the structure having the same general contour as the lead edge of the tube, corresponding to the end of the proton range; and (2) erosion of the tube in the region where the dark band intersects the specimen surface. At 1000× magnification [Fig. 3 (a)], the dark band is resolved into a large number of discrete cavities located within the grains of the aluminum, while a nearly continuous network of cavities and linked cavities delineates the grain boundaries. The maximum cavity diameter is approximately 2.5 μm. Many of the cavities within the grains are associated with precipitate particles. These precipitates were

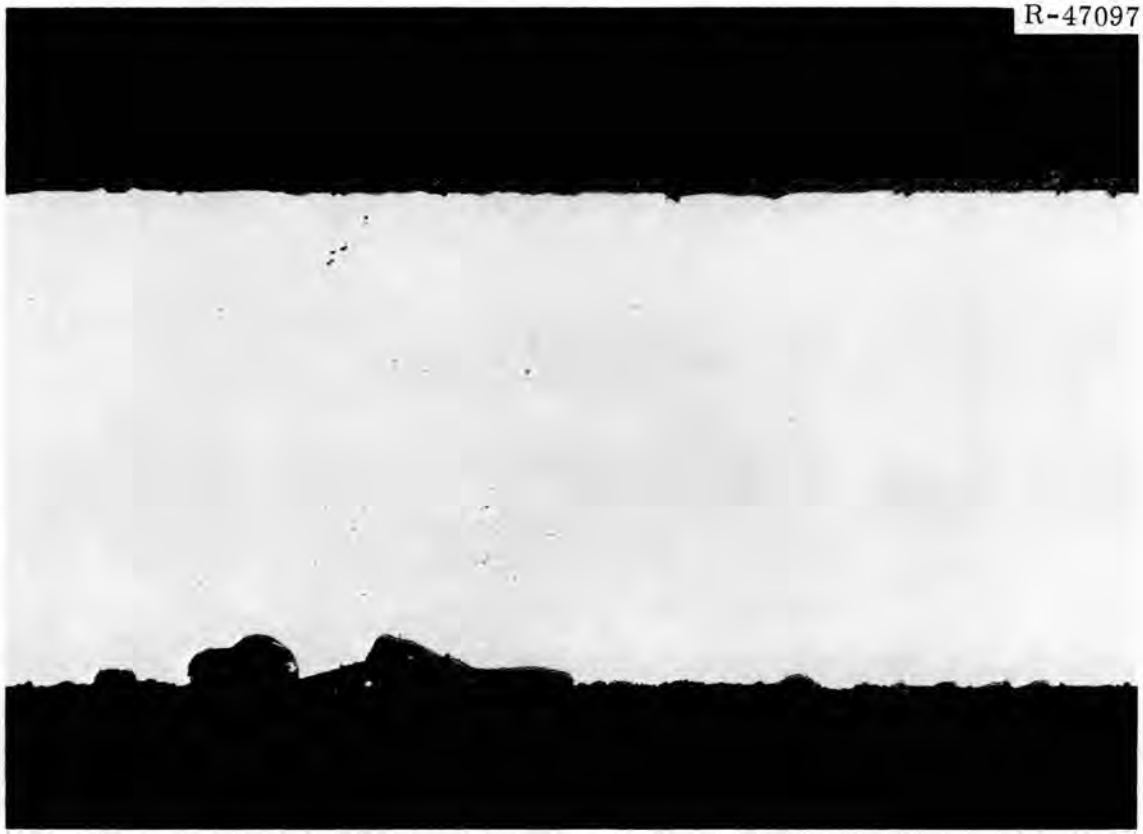

Fig. 2. Cross-Section Through Aluminum Tube at the End of the Proton Range. Showing Region Darkened By Band of Hydrogen Bubbles. As-Polished. 100×.

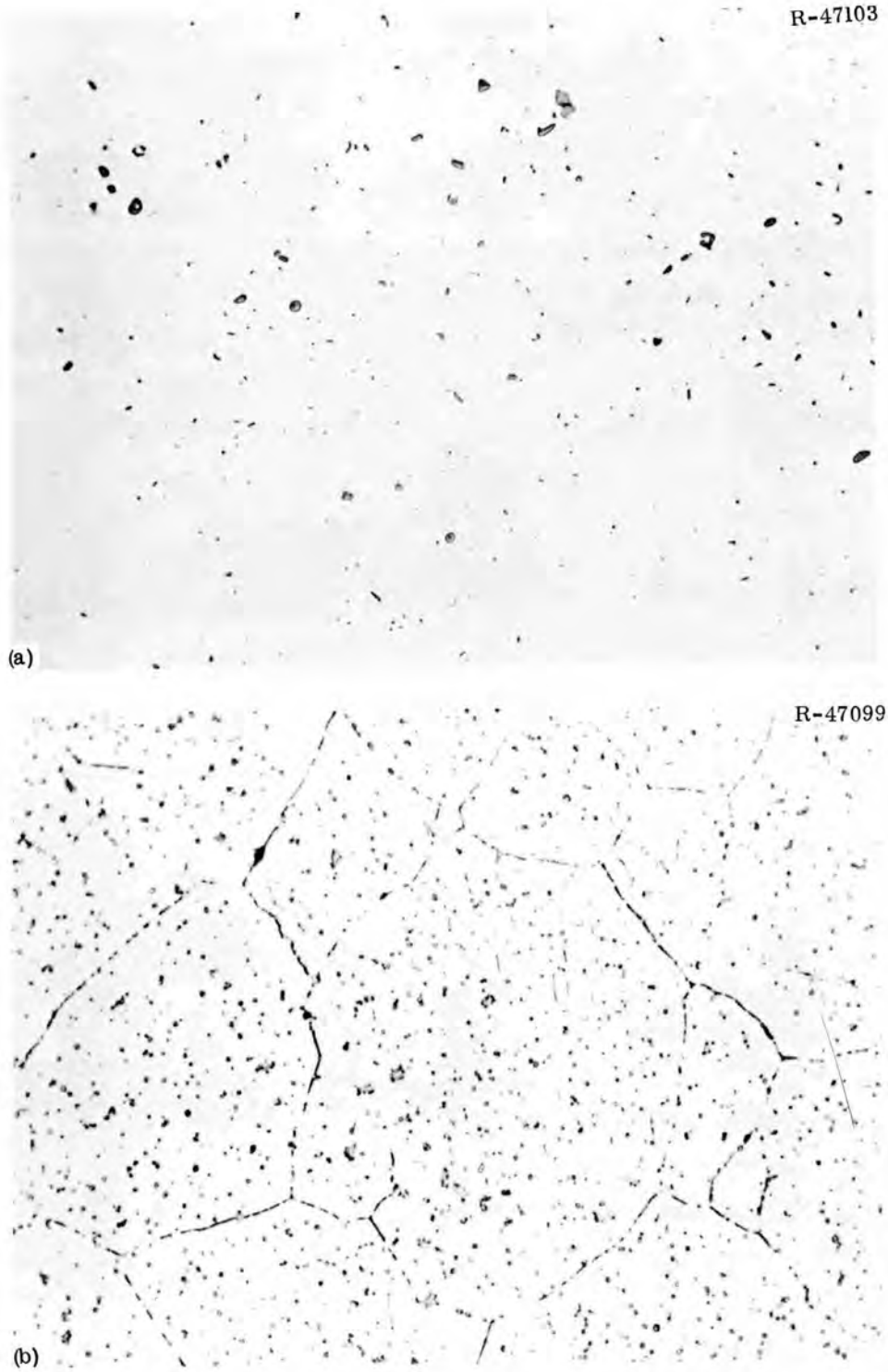

Fig. 3. Comparison of Regions of the Microstructure Shown in Fig. 2 at Higher Magnification. (As-Polished). (a) Region Containing Hydrogen Bubbles. (b) Region Not Bombarded by Protons. 1000×.

probably present before bombardment, since the microstructure in a region through which the protons did not pass also contained similar precipitates [Fig. 3 (b)].

The effect of annealing the region near the end of the proton range for 20 hr at 600 °C is shown in Fig. 4. Growth and possibly coalescence of the cavities occurred, leading to a microstructure containing cavities ranging in size from the lower limit of resolution of the microscope up to 0.025 cm in at least one dimension. The areas adjacent to the original dark band frequently exhibited cavities on grain boundaries. In some areas within the original band, grain boundaries have completely separated.

DISCUSSION

It is apparent from the evidence presented above that the large quantities of hydrogen injected into the aluminum beam extraction system of the ORNL 86-in. cyclotron had two effects: (1) cavities formed on grain boundaries, at pre-existing precipitate particles, and perhaps in the matrix of the aluminum at the end of the proton range and (2) erosion of the aluminum was accelerated at the surfaces where these cavities existed. The cavities are almost certainly hydrogen-filled bubbles stabilized by internal gas pressure at the operating temperature of the tubing. Voids produced by neutron irradiation of aluminum never occur on grain boundaries[4] and voids have almost always been observed to shrink in annealing. Annealing causes the cavities in this component to grow. Ells and Evans[5] have shown that hydrogen bubbles can form in aluminum alloys as a result of cyclotron proton bombardment at less than 100 °C, and that less than 1 wt ppm of H_2 is required to form bubbles in Mg—Al alloys. However, they demonstrated that the size and number density of bubbles observed vary with bombardment temperature and thus depends strongly upon hydrogen and vacancy diffusion, so that presumably the rate of gas injection might be an important parameter in affecting the final bubble distribution. Hence, Ells and Evans[5] results cannot be compared directly with these results.

Further discussion requires some estimate of the operating temperature of the tubing. From other measurements we know that if the entire

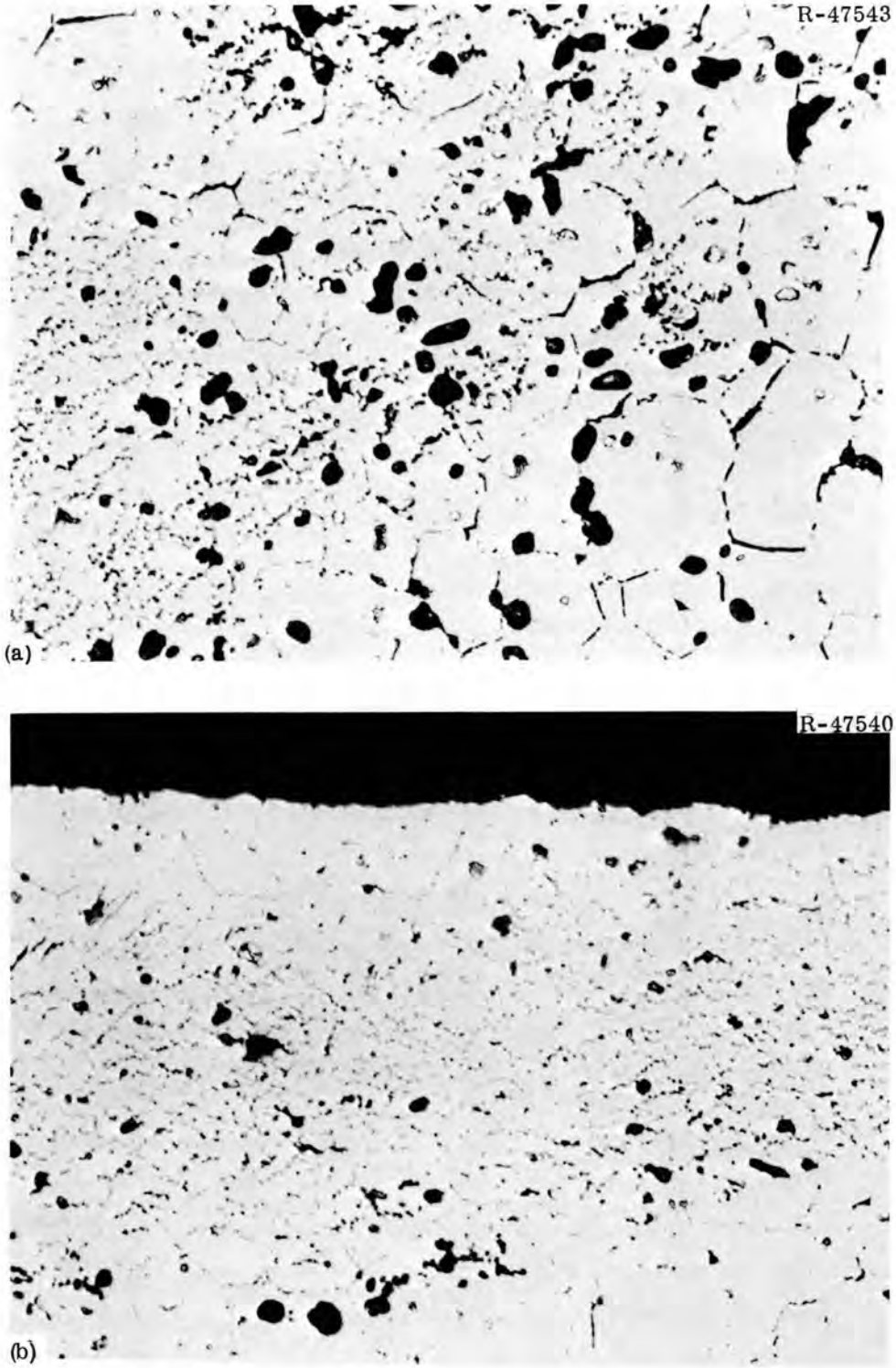

Fig. 4. Regions Near End of Proton Range After Annealing for 20 hr at 600°C. As-Polished. (a) Near the center of the band and (b) near the edge of the band. 500×.

circulating beam in the cyclotron tank (approx 200 μa of 22.5 MeV protons) impinges normally on a flat sheet of aluminum, it covers an area of almost 5 cm^2. Since the deflector normally intercepts only the fringe beam, the maximum probable current density on the tube os 40 $\mu a/cm^2$. The temperature difference between the tube wall in contact with the water and outer portion of the tube which is heated by the slowing particles is estimated for steady state conditions to be:

$$\Delta T = \frac{q\,\Delta X}{kA} \cong 13\,^\circ C\,, \qquad (1)$$

where $k = 48$ cal · sec^{-1} cm^{-1} $^\circ C^{-1}$, the thermal conductivity of aluminum,[7]

$$q = 22.5 \text{ MeV} \times 200\ \mu a \times 2.389\ \frac{\text{cal}}{\text{sec} \cdot \mu a \cdot \text{MeV}}\,,$$

$\Delta X = 0.26$ cm, the tube wall thickness,

$A = 5$ cm^2, the surface area.

We have ignored the variation of proton energy loss rate along its path,[6] and we have conservatively taken ΔX to the full tube wall thickness. The resultant temperature gradient has not been obtained for the correct geometry, but it gives the order of magnitude of the effects to be expected. Ignoring the nonuniformity of the beam distribution, it is unlikely that the specimen operated at a temperature more than a few degrees in excess of the nonboiling coolant water temperature.

At 100 °C, if the diffusion coefficient of hydrogen in aluminum is given by[5]

$$D = 0.21 \exp\,(-10{,}900/RT) \qquad (2)$$

D is 8×10^{-8} cm^2/sec, and a single hydrogen atom makes approximately 10^8 jumps/second.[8] Hence, hydrogen may be considered to be very mobile at the bombardment temperature. However, vacancies and interstitials are also produced by decelerating protons as they pass through the aluminum, and the production rate is highest near the end of the proton range.[6] The gas bubbles observed are therefore probably due to the combined supersaturations of both hydrogen and vacancies. Because

the ion current density incident upon the tube varied with time in an unknown manner, it would be meaningless to attempt to estimate the absolute value of the supersaturation.

Ells and Evans[5] have enumerated the competing processes which account for the growth or disappearance of a band of hydrogen bubbles during postbombardment annealing. The final equilibrium condition is clearly solid aluminum containing an equilibrium number of thermal vacancies and dissolved hydrogen in equilibrium with the environment. However, intermediate steps are governed by kinetic processes involving diffusion of vacancies between the bubbles and other sources and sinks, and the diffusion of hydrogen between bubbles and the free surfaces. During this process, the bubbles attempt to maintain an equilibrium concentration of vacancies and hydrogen in the surrounding matrix, as determined by capillarity considerations.[9] The equilibrium gas pressure within the bubbles, $2\gamma/r$, may be combined with the ideal gas law to give the following relation:

$$r^2 = \frac{3nRT}{8\gamma\pi} \tag{3}$$

where r is bubble radius, n is the number of moles of gas in the bubble, γ is surface tension, R is the gas constant, and T is absolute temperature. Hence, increasing the temperature ought to cause bubbles to tend to acquire vacancies and grow at constant gas content, and if supersaturated gas is also being acquired, further growth is possible by increasing n. Normal Ostwald ripening, the growth of large bubbles at the expense of their smaller neighbors, is a concurrent process during elevated temperature annealing which complicates the situation.

The accelerated corrosion at the surfaces above the band of bubbles is probably affected by the high density of bubbles along the grain boundaries; even if the grain boundaries were oxidized at the same rate as the matrix, eventually the boundary regions would be completely dissolved before the bulk of the grain might be substantially affected, causing the grains to literally fall out or be washed out by the coolant water stream.

A second possible cause of the accelerated corrosion in this region is the ionization of water by protons. Above proton energies of a few

keV the rate of ionization decreases with increasing proton energy; thus, this effect should be strongest near the end of the particle range. The free OH^- radicals produced in this manner might then react with the exposed aluminum surface to produce the observed corrosion. A similar effect was previously observed for Inconel target sheaths exposed to the ORNL 86-in. cyclotron beam in contact with water.[10]

The tube failed while operating under approximately 100 psi of internal water pressure. By simple analysis, the maximum normal stress in the flats where failure occurred could not have exceeded about $\frac{P}{2}$, where P is the water pressure (100 psi), about two orders of magnitude below the yield strength of 1100 aluminum near room temperature. It is, therefore, quite unlikely that the externally applied stress had any direct effect on the undamaged portion of the tube. Certainly no gross straining of the tube occurred, as can be seen in Fig. 1. Further, the macroscopic cross-sectional area was not sufficiently reduced by erosion to significantly increase the stress calculated on a macroscopic basis. The cause of the failure, is, however, intimately associated with the bubbles. We can envision at least two failure mechanisms, both of which probably occur simultaneously to some extent. These mechanisms can interact and be mutually enhancing.

1. Increased stress on the grain boundaries due to the high concentration of bubbles on the boundaries. Examination of Fig. 2 shows that a large fraction of the available grain boundary area was occupied by bubbles. In some regions, the grains were completely separated by linked bubbles; such boundaries were not capable of bearing stress, and consequently, the stress on surrounding areas of the boundaries was greatly increased by the simple reduction in the microscopic cross-sectional area thus effected. The tip of an array of linked bubbles is essentially the tip of a crack, and the stresses around the crack tip are also subject to the intensification considerations common to fracture mechanisms. Local deformation along grain boundaries would then be a mechanism for propagating the failure.

2. Failure by growth and linking of bubbles. The bubbles in the process of forming by the deposited hydrogen and the excess vacancies might simply have grown until a continuous passageway for water formed

between the inside and outside of the tubing, thus giving rise to pinhole leaks. However, in the presence of a tensile stress component, σ, a gas bubble is unstable and grows without limit if[11]

$$r > \frac{4}{3\sqrt{3}} \frac{\gamma}{\sigma} . \qquad (4)$$

For $\gamma \cong 10^3$ dynes/cm and $\sigma = 6.9 \times 10^6$ dynes/cm^2 (about 100 psi) the critical radius above which bubbles grow without thermodynamic barrier is approximately 1.1×10^{-4} cm. Thus, the applied stress is sufficient to cause growth of the largest observed bubbles (approx 1.2×10^{-4} cm radius) until they impinge, even through it is not a large stress from the standpoint of normal deformation mechanics. Within the limits of uncertainty of this analysis, the coincidence between the calculated critical bubble radius and the observed maximum is striking. It suggests that bubbles grow by normal diffusion processes until the critical radius is reached, and then in some areas, catastrophic growth leading to failure occurs. The thermal cycling from daily machine shutdowns may also be important, since the bubbles may equilibrate overnight by accommodating more hydrogen, which would create a pressure greater than the equilibrium pressure when the temperature rose during the next startup.

Because so little is known about the operating conditions of the tube, these remarks must be considered speculative.

SOLUTION TO THE PROBLEM

Recent experience with neutron-irradiated aluminum alloys has shown that the age-hardened 6061 alloy with its fine dispersion of Mg_2Si precipitate particles is more resistant to the formation of neutron-irradiation induced voids than solid solution alloys such a 1100 aluminum.[12] While the ratio of gas atom to vacancy supersaturation is greater in the ion-bombarded material than in the neutron-irradiated material, it is likely that the precipitate particles may inhibit gas bubble nucleation. At the least, we expect that a number of gas bubbles might nucleate on the Mg_2Si particles, trapping the gas at sites away from

the grain boundaries. A trial deflector might be constructed of 6061-T6 aluminum, operated for a period comparable to that required to cause failure of an 1100 aluminum tube, and examined metallographically before its sale.

CONCLUSIONS

During the operation of the ORNL 86-in. cyclotron, a beam of 22.5 MeV protons which is stopped in a water-cooled 1100 aluminum tube of the beam extraction system is responsible for the degradation and failure of the tubing. Metallographic examination has demonstrated that:

1. Hydrogen bubbles form preferentially on grain boundaries and precipitate particles, although bubbles are also observed in the matrix of the tube. The bubbles are only observed in the region where the hydrogen is deposited.

2. Accelerated wall thinning of the tube occurs in the region where the hydrogen bubbles form, probably by the removal of entire grains on whose boundaries a very high bubble density exists.

3. Pinhole leaks form in the region of the tube where the bubbles are observed. This mode of failure is associated with the presence of the bubbles, but the exact mechanism of failure cannot be ascertained.

4. Annealing the tubing for 20 hr at 600°C causes the gas bubbles to grow.

ACKNOWLEDGMENTS

We wish to thank S. E. Spencer for the metallography. We also thank J. O. Stiegler and F. W. Wiffen for reviewing this manuscript, Susan Price for typing the draft, and Carol Kilgore for the final typing and preparation of the report for reproduction.

REFERENCES

1. J. L. Brandt, "Properties of Pure Aluminum," p. 26 in Aluminum, vol 1, ed. by K. R. Van Horn, American Society for Metals, Metals Park, Ohio, 1967.

2. K. Farrell, A. Wolfenden, and R. T. King, "The Effects of Irradiation Temperature and Preinjected Gases on Voids in Aluminum," Radiat. Eff. 8, 107–114 (March 1970).

3. J. P. Janni, Calculations of Energy Loss, Range, Pathlength, Straggling, Multiple Scattering, and the Probability of Inelastic Nuclear Collisions for 0.1 to 1000 MeV Protons, Technical Report No. AFWL-TR-65-150, Air Force Weapons Laboratory, Kirtland Air Force Base, New Mexico (September 1966)

4. J. O. Stiegler, K. Farrell, C.K.H. DuBose, and R. T. King, "High-Fluence Neutron-Irradiation Damage in Aluminum," pp. 215–232 in Radiation Damage in Reactor Materials Vol. II (Proceedings of a Symposium, Vienna 2–6 June 1969), International Atomic Energy Agency, Vienna, 1969.

5. C. E. Ells and W. Evans, "The Agglomeration of Hydrogen in Aluminum," Trans. AIME 227, 438 (April 1963).

6. R. T. King, On the Production of Displacement Damage by Light Ions, ORNL-TM-3013 (1969).

7. G. Shortley and D. Williams, Elements of Physics, 2nd Ed., Prentice-Hall, Englewood Cliffs, N.J., p. 290 (1955).

8. P. G. Shewmon, Diffusion in Solids, McGraw-Hill, New York, p. 43 (1963).

9. W. W. Mullins, "Morphologies Governed by Capillarity," p. 43 in Metal Surfaces, American Society for Metals, Metals Park, Ohio, 1962.

10. J. B. Ball, ORNL, private communication.

11. R. S. Barnes and R. S. Nelson, "Theories of Swelling and Gas Retention in Reactor Materials," pp. 225–267 in Radiation Effects Met. Soc. Conf. 37 ed. by W. F. Sheely, Gordon and Breach, New York, 1967.

12. R. T. King, A. Jostsons, and K. Farrell, "Examination of the Irradiated 6061 Aluminum HFIR Target Holder Sleeve," to be published.

INTERNAL DISTRIBUTION

1–3. Central Research Library
4. ORNL – Y-12 Technical Library Document Reference Section
5–15. Laboratory Records Department
16. Laboratory Records, ORNL RC
17. ORNL Patent Office
18. G. M. Adamson, Jr.
19. J. B. Ball
20. E. E. Bloom
21. J. A. Cox
22. F. L. Culler
23. J. E. Cunningham
24. W. W. Davis
25. D. Fahr
26. K. Farrell
27. J. H Frye, Jr.
28. R. E. Gehlbach
29. W. O. Harms
30–32. M. R. Hill
33. F. J. Homan
34. A. Jostsons
35. C. R. Kennedy
36–56. R. T. King
57. B.T.M. Loh
58–68. E. L. Long, Jr.
69. R. S. Lord
70. W. R. Martin
71. H. E. McCoy, Jr.
72. C. J. McHargue
73. E. Newman
74. O. S. Oen
75. P. Patriarca
76. A. W. Riikola
77. A. C. Schaffhauser
78–88. M. R. Skidmore
89. S. E. Spencer
90. R. L. Stephenson
91. J. O. Stiegler
92. R. W. Swindeman
93. D. B. Trauger
94. J. E. Van Cleve
95. R. D. Waddell, Jr.
96. J. R. Weir, Jr.
97. F. W. Wiffen
98. A. Wolfenden
99. J. W. Woods
100. F. Young

EXTERNAL DISTRIBUTION

101. H. B. Barkley, Jr., NASA, Plumbrook Reactor Facility, Sandusky, OH 44870
102–112. J. E. Beaver, University of Miami Medical School, Department of Nuclear Medicine, Miami, FL 33100
113–114. E. G. Case, Director, Division of Reactor Standards, AEC, Washington, DC 20545
115. J.G.Y. Chow, Brookhaven National Laboratory, 29 Cornell Avenue, Upton, Long Island, NY 11973
116. T. T. Claudson, Hanford Engineering Development Laboratory, P.O. Box 999, Richland, WA 99352
117. W. Compas, United Nuclear, New Haven, CT 06500
118. D. F. Cope, RDT, SSR, AEC, Oak Ridge National Laboratory, Oak Ridge, TN 37830
119. G. W. Cunningham, Division of Reactor Development and Technology, AEC, Washington, DC 20545
120. J. A. DeMasty, Westinghouse Electric Corporation, Astronuclear Laboratory, Pittsburgh, PA 15236
121–125. Executive Secretary, Advisory Committee on Reactor Safeguards, AEC, Washington, DC 20545

126. E. A. Evans, Hanford Engineering Development Laboratory, P.O. Box 999, Richland, WA 99352
127. C. R. Finfgeld, Department of Physics, Roanoke College, Salem, VA 24153
128. E. E. Gruber, Argonne National Laboratory, 9700 South Cass Avenue, Argonne, IL 60439
129. D. H. Gurinsky, Brookhaven National Laboratory, 29 Cornell Avenue, Upton, Long Island, NY 11973
130. R. L. Huntoon, Savannah River Laboratory, Aiken, SC 29801
131. G. E. Korth, Idaho Nuclear Corporation, P.O. Box 1845, Idaho Falls, ID 83401
132. D. Kramer, Atomics International, P.O. Box 309, Canoga Park, CA 91304
133. A. R. Landgrebe, AEC, Washington, DC 20545
134. P. J. Levine, Westinghouse Advanced Reactor Division, Waltz Mill Site, Madison, PA 15663
135. J. J. Lombardo, SNPO, NASA, Lewis Research Center, 21000 Brookpark Road, Cleveland, OH 44135
136. G. R. Love, Union Carbide Corporation, P.O. Box 5928, Greenville, SC 29601
137. C. L. Matthews, RDT, OSR, AEC, Oak Ridge National Laboratory, Oak Ridge, TN 37830
138. E. Miller, NASA, Lewis Research Center, 21000 Brookpark Road, Cleveland, OH 44135
139–141. P. A. Morris, Director, Division of Reactor Liscensing, AEC, Washington, DC 20545
142. M. Oselka, Argonne National Laboratory, Cyclotron, Building 211, Argonne, IL 60439
143. N. H. Packan, Institut für Material und Festkorperforschung Kernforschungszentrum Karlsruhe 75 Karlsruhe (WEDERSTRASSE 5) West Germany
144. H. Pearlman, Atomics International, P.O. Box 309, Canoga Park, CA 91304
145. W. E. Ray, Westinghouse Advanced Reactor Division, Waltz Mill Site, Madison, PA 15663
146. L. S. Reubenstein, Division of Reactor Development and Technology, AEC, Washington, DC 20545
147. J.A.L. Robertson, Head, Reactor Materials Branch Chalk River Nuclear Laboratories, Atomic Energy of Canada, Ltd., Chalk River, Ontario, Canada
148. P. G. Shewmon, Argonne National Laboratory, 9700 South Cass Avenue, Argonne, IL 60439
149. Sidney Siegel, Atomics International, P.O. Box 309, Canoga Park, CA 91304
150. W. F. Sheely, Hanford Engineering Development Laboratory, P.O. Box 999, Richland, WA 99352
151. J. M. Simmons, Division of Reactor Development and Technology, AEC, Washington, DC 20545
152. E. E. Sinclair, Division of Reactor Development and Technology, AEC, Washington, DC 20545
153. D. K. Stevens, Division of Research, AEC, Washington, DC 20545

154. E. F. Sturcken, Savannah River Laboratory, Aiken, SC 29801
155. A. Taboada, Division of Reactor Development and Technology, AEC, Washington, DC 20545
156. A. Van Echo, Division of Reactor Development and Technology, AEC, Washington, DC 20545
157. C. E. Weber, Division of Reactor Development and Technology, AEC, Washington, DC 20545
158. G. A. Whitlow, Westinghouse Advanced Reactor Division, Waltz Mill Site, Madison, PA 15663
159. K. M. Zwilsky, Division of Reactor Development and Technology, AEC, Washington, DC 20545
160. Laboratory and University Division, AEC, Oak Ridge Operations
161–162. Division of Technical Information Extension